RSC Advances

PAPER

View Article Online
View Journal | View Issue

Cite this: *RSC Adv.*, 2021, **11**, 14996

A highly efficient microwave-assisted synthesis of an LED-curable methacrylated gelatin for bio applications†

Sahar Abdollahi Baghban, Morteza Ebrahimi,* Shadab Bagheri-Khoulenjani and Manoucher Khorasani

This study deals with the development of an LED-curable methacrylated gelatin (GelMA) synthesis *via* microwave (MW) irradiation with a reaction and purification time-, energy-, and methacrylation reagent-saving approach. To investigate the efficiency of MW irradiation in GelMA synthesis, characteristics of the GelMAs prepared by using glycidyl methacrylate (GMA) or methacrylic anhydride (MA) *via* the MW-assisted (MWA) method were compared comprehensively with those synthesized *via* the conventional heating method. Moreover, MWA reaction conditions were optimized in terms of methacrylation reagent concentrations (*C*), reaction time (*t*), and MW power (*P*). Characterization and assessment of the GelMAs were conducted with ^{1}H NMR, FT-IR, and Raman spectroscopy along with physical-mechanical, thermal, and hydrophilicity analysis. The results demonstrated that the MWA synthesized GMA–GelMA hydrogels were possessed of increased methacrylation degree (MD), gel fraction (GF), tensile strength (TS), elongation at break (EB), glass transition temperature (T_g), and water contact angle (WCA) as well as decreased swelling degree (SD) values in comparison to those of MA–GelMA and GMA–GelMA hydrogels prepared *via* the MWA and conventional method, respectively. Enhanced properties of the MWA synthesized GMA-hydrogels suggested an effective methacryloyl conjugation leading to a greater amount of covalent crosslinking density justified by the dipolar moment calculations. Optimal GMA *C*, *t*, *P*, and purification time for a highly crosslinked GelMA hydrogel (MD: 96.1%, GF: 98.3%, SD: 10.11%, TS: 6.7 MPa, EB: 175.2%, T_g: 75.34 °C, and WCA: 72.22°) were found to be a 5 times molar excess over the primary amine groups of gelatin, 5 min, 500 W, and 24 h, respectively. Thus, the optimized MW conditions offer a promising green method to prepare GelMAs for bio applications.

Received 16th February 2021
Accepted 10th April 2021

DOI: 10.1039/d1ra01269j

rsc.li/rsc-advances

Introduction

Nowadays, gelatin-derived hydrogels are widely employed as interesting renewable sources for mimicking bio tissues, making wound dressings and drug delivery beds, fabricating food coatings, *etc.*[1–4] Hydrogels are considered insoluble three-dimensional (3D) polymeric networks capable of swelling and retaining a large volume of water.[3–6] Gelatin is a natural water-soluble protein that offers an attractive choice for preparing bio-hydrogels because of its outstanding properties including biocompatibility, biodegradability, low price, abundance, suitable processing and modifying capability, high transparency, digestibility, and appropriate film- or gel-forming ability.[2,4–8] Despite all the benefits of pure gelatin, high fragility and low mechanical strength, high moisture absorption, low proteolytic degradation resistance, and relatively high thermal sensitivity in comparison with synthetic polymers are regarded as its drawbacks.[3–6,9–12] Several methods have been utilized to solve some of the abovementioned shortcomings namely chemical, physical and enzymatic crosslinking, plasticizing, compounding with other polymers, laminating, salt addition, as well as reinforcing with micro and nano-sized particles.[8–15] It was reported that chemical crosslinking methods have the highest efficiency to improve the mechanical strength of gelatin. In this regard, numerous chemical crosslinkers such as genipin, starch dialdehyde, formaldehyde, glutaraldehyde, diphenyl phosphoryl azide, glyoxal and different polyepoxides, carbodiimides, polysaccharides, diisocyanates, and natural phenolic compounds have been introduced to make irreversible covalent bonds between gelatin chains.[5,6,8–15] The possible cytotoxic side effects and uncontrollable crosslinking rate of these chemicals are the major disadvantages that cannot be ignored.[8–12,16–20] In a new approach first introduced by Van Den Bulcke and his co-workers, gelatin was turned into a light-curable protein *via* a one-step methacrylation reaction.[16–18] Aqueous methacrylated gelatin (GelMA) solution can be photo-crosslinked and transformed into an insoluble network within several seconds to

Department of Polymer and Color Engineering, Amirkabir University of Technology, 350 Hafez Ave., 15875-4413 Tehran, Iran. E-mail: ebrahimi@aut.ac.ir

† Electronic supplementary information (ESI) available. See DOI: 10.1039/d1ra01269j

minutes under ultraviolet (UV) or visible light irradiation in the presence of photoinitiators.[8–12,16–19,21–23]

Photo-curing has received considerable attention as an excellent method to develop the hydrogels due to the fast crosslinking at mild conditions (in aqueous environments, neutral pH, and at ambient temperature) and being environmentally-friendly (no solvent emission and low energy consumption).[18,20,22,24–26] In the conventional GelMA synthesis, the primary amine groups existing on the lysine (LY) and hydroxylysine (HLY) amino acids of gelatin react directly with anhydride group of methacrylic anhydride (MA) at 50–60 °C in an aqueous media for 1–10 h resulting in the GelMAs with various methacrylation degrees (MDs).[21,22,25–31] It was stated that highly methacrylated gelatin can be almost only achieved in the conventional methacrylation method by using an excess amount of MA (up to 30 times molar excess) over the estimated primary amine groups of gelatin during a quite long time (10 h).[21,22,31–35] In this method, further increasing the reaction temperature to decrease the reaction time is not practical because of the MA hydrolysis probability.[22,25] Besides, the unreacted MA monomers and side products must be removed at the end of the methacrylation reaction due to their cytotoxic effects on the alive cells. The complete washing and purification usually last for 1–6 weeks.[20–25,33–38] Consequently, increasing the MA concentration, time, and temperature are not proper solutions. Up to now, the improvement of the GelMA synthesis and purification procedures is still an underlying challenge for the hydrogel field. According to several publications over the past 30 years, one of the most important methods to increase the chemical reaction rate is the irradiation of microwave (MW).[37,39–41] Based upon the widespread studies, the main advantages of the MW-assisted (MWA) synthesis over the conventional heating methods include the reaction time and side products reduction, uniform and homogeneous reaction, selectiveness, and subsequently higher yields under milder reaction conditions which permit energy and time saving towards the green and sustainable chemistry.[39–43] Irmak *et al.* obtained GelMAs by coupling MA and gelatin under the MW condition and expressed some benefits over the conventional method like the significant reduction of the reaction and purification time as well as the required MA concentration due to the increased reaction efficiency. They investigated the effects of varying the MW power and MA concentration on the MD of GelMAs by using ^{1}H-NMR analysis.[37] Besides, some of the investigations have also prepared GelMAs by using a less known methacrylation reagent, glycidyl methacrylate (GMA) under the conventional heating method.[19,25]

To the authors' best knowledge, no study has been performed on the possibility of the GelMA synthesis using GMA under the MW irradiation. Additionally, there is no report on comparing the methacrylation of gelatin using GMA and MA under the MW or conventional conditions. In this study, different photo-reactive GelMAs were synthesized by the coupling reaction of amine groups of gelatin with GMA and MA using both the MWA and conventional methods. Then, the GelMA synthesizes were proved by characterization analysis. In the following, synthesized GelMAs were LED-cured to examine the achieved hydrogels and compare synthesis methods.

Materials and methods

Materials

Gelatin (Type A, bloom strength: 300, isoelectric point: 9) isolated from porcine skin by an acidic process in the form of powder was supplied by Sigma-Aldrich. The pH at 25 °C and viscosity of a 15% (w/v) gelatin solution at 50 °C were 5.69 and 6 mPa s, respectively. This gelatin had 0.36 mmol amino groups per gram, arising from the LY and HLY residues. Methacrylic anhydride (MA) (purity: ≥94%, contains ~2000 ppm topanol A as an inhibitor), glycidyl methacrylate (GMA) (purity: ≥97.0%, contains ~100 ppm hydroquinone monomethyl ether as an inhibitor), gelatin, and phosphate-buffered saline tablets (PBS, pH: 7.4) were purchased from Sigma-Aldrich and used as received without further purification. The water-soluble visible absorbing type I photoinitiator, VA-086 (2,2′-azobis[2-methyl-*N*-(2-hydroxyethyl)propionamide]) was provided kindly by FUJI FILM Wako Pure Chemical Industries Ltd.

Synthetic procedures

GelMAs were synthesized *via* the conventional and MWA methods. The details of these methods are explained in the following sections.

Conventional GelMA synthesis method. GelMAs were synthesized based on a conventional method reported by Benton *et al.*[21,44] In this method, 10 g of gelatin was dissolved completely in 100 mL of PBS solution (10% (w/v)) at 50 °C and mixed for 1 h. Then, 5 and 10 molar excess of GMA and MA over the primary amino groups present along the gelatin backbone (0.36 mmol g^{-1}) were added dropwise at a constant rate of 0.5 mL min^{-1} at 40 °C into the gelatin solution. During the reaction, the mixture was stirred vigorously using a mechanical stirrer with constant stirring at 400 rpm. The reaction was allowed to proceed for 4 h at 50 °C in dark media. The reaction mixture was cooled to ambient temperature by diluting the solution with 1 L double distilled water (DDW) to terminate the methacrylation reaction.

Microwave-assisted GelMA synthesis method. GelMAs were synthesized under the MW irradiation using the same amounts of materials used in the conventional method. Gelatin powder was dissolved in PBS solution (10% (w/v)) at 50 °C and stirred for 1 h to attain a 10% (w/v) clear solution. This solution was poured into a 250 mL round bottom flask placed on the turntable plane in an MW oven (WBFY-201, Zhengzhou Keda Machinery and Instrument Equipment (ZZKD) Co., China, Type: Electrolyzer) equipped with microcomputer temperature control. GMA and MA were added dropwise at 0.5 mL min^{-1} into the flask using a syringe under stirring in the MW oven. The final mixtures were exposed to the MW irradiation for 1, 5 and 10 min with different powers (100, 500 and 1000 W) according to Table S1.† The irradiation was stopped every 30 s to remain the mixture temperature at 50–60 °C. The pH was adjusted to 7.4–7.8 with NaOH solution (0.1 M) as needed. Fig. 1

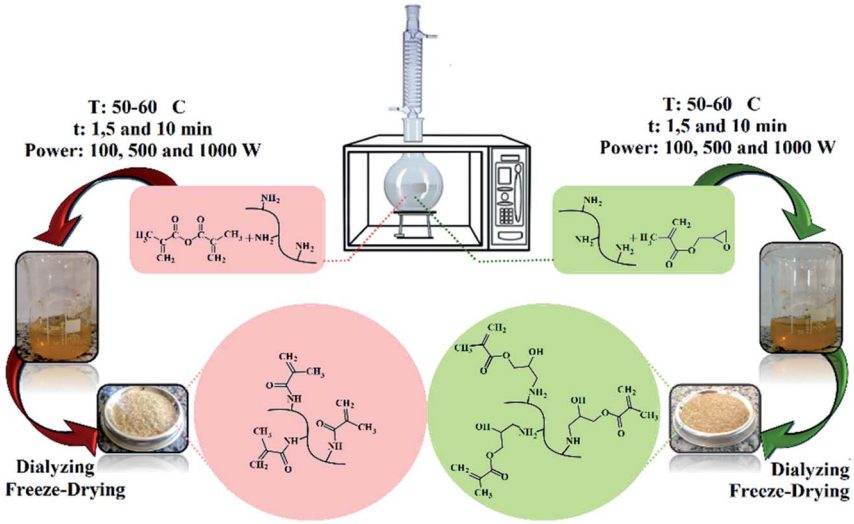

Fig. 1 MWA synthesis and purification steps of GelMAs by GMA and MA.

illustrates the schematic MWA synthesis processes of GelMAs. Details of 40 formulations prepared and named as **T-W-X-Y-Z** (*e.g.* MW-G-5-1-100) were given in Table S1.†**T**, **W**, **X**, **Y** and **Z** mean:

T: synthesis method (C: conventional and MW: microwave)

W: methacrylation reagent (G: GMA and M: MA)

X: methacrylation reagent concentration (5 or 10 times molar excess of GMA or MA over the primary amino groups of gelatin)

Y: methacrylation time (1, 5 or 10 min)

Z: MW power (100, 500 or 1000 W)

The pH value of the obtained GelMA solutions was measured by laboratory pH meter (Knick 765), after 1 h cooling at room temperature. The GelMA solutions were transferred to dialysis membranes (10 kDa molecular weight cutoff) and dialyzed against the flowing deionized (DI) water for 1 day at 25 °C to remove unreacted GMA, MA, and by-products. DI water was changed regularly every 8 h. The clear yellowish viscous dialyzed GelMA solutions (see Fig. S1 ESI section†) were subjected to freeze-drying under reduced pressure leading to a purified solid powder (see Fig. S2 in ESI†). The freeze-dried GelMAs were stored at room temperature in a dark environment before use.

LED-curing of GelMA solutions. Photo-crosslinking of aqueous GelMA solutions was performed under the LED irradiation in the presence of a water-soluble photoinitiator, VA-086 (Lambda max: 374 nm (see Fig. S3 in ESI†)). According to the previous reports, the optimum VA-086 concentration is equivalent to 0.5–1.0 wt% concerning bioactivity (cell viability), curing kinetics, and gel strengths.[44–49] The film-forming solutions were prepared by dissolving 1.0 wt% VA-086 into 15% (w/v) GelMA solution in distilled water (DW) under dark media. The prepared solutions were applied and spread uniformly on glass substrates by 240 μm wired bar hand applicator to achieve 30 μm dry films. Then, irradiation was immediately conducted under a custom-made blue LED light source at room temperature (25 ± 1 °C) for 90 s at a distance of 10 cm below the outer shield of the LED light source. The spectral power distribution of the light source was measured in the range of 230–850 nm using an OHSP-350UV ultraviolet visible spectrometer (Hangzhou Hopoo Light & Color Technology Co., China) calibrated against an international standard set according to ISO/ASTM 52628–20. The light intensity of LED was found to be in the range of 37–77 mW cm^{-2} in a wavelength range of 370–420 nm as displayed in Fig. S4.† For some characterizations, the dry films were peeled off from the substrate and cut into small pieces using a conventional scissor. After that, the films were kept in a container at room temperature (25 ± 2 °C) and 45% RH before analysis.

Characterization and measurements

Synthesized GelMAs and their photo-crosslinked films were subjected to different characterization and evaluation tests to assess the gelatin methacrylation.

Proton nuclear magnetic resonance (^{1}H NMR) spectroscopy. The MD of prepared GelMAs expressed as the percentage of the primary amine groups coupled with GMA or MA was quantified using Bruker INOVA ^{1}H NMR spectrometer (Germany). 15 mg of samples were completely dissolved in 10 mL deuterium oxide (Sigma-Aldrich) at 35 °C and three ^{1}H NMR spectra were recorded from each sample at a frequency of 500 MHz with 32 scans and a recycle delay of 3 s using a single axis gradient inverse probe. Baseline correction was applied before calculating the integral areas of each interest peaks.

Fourier transform infrared (FT-IR) spectroscopy. The FT-IR spectrometry analyses were carried out by an FT-IR BOMEM MB-Serie spectrometer to confirm the synthesis of GelMAs. The FT-IR spectra were recorded in the range of 4000 to 400 cm^{-1} in the transmission mode acquired from 20 scans at a resolution of 4 cm^{-1}.

Raman spectroscopy. Raman spectra of pure gelatin and GelMA were attained using a Horiba Xplora plus confocal Raman microscope (France) equipped with a 785 nm laser and

a Syncerity OE detector at room temperature (acq. time (s): 4, slit: 100 μm, ICS correction: off, grating: 1200 (750 nm)).

Swelling degree and gel fraction. The swelling degree (SD) or water uptake capability of the synthesized hydrogels was measured by the gravimetric method based on the standard BS EN 13726-1:2002. Each of the prepared films was cut uniformly to 2 × 3 cm pieces maintained in a desiccator with silica gel at 0% RH for 24 h. Then, they were weighed (m_o) using a calibrated balance to the nearest 0.0001 g followed by submerging in a beaker containing 80 mL of DW at 25 °C for 2 min. Afterward, the soaking films were wiped with filter paper to remove the water adhered to the surface of the specimens and reweighed (m_1). Another piece of each sample was immersed for 48 h in the beaker containing DW to extract non-joint polymer chains. Then, all of the beaker content was poured on a piece of filter paper followed by washing and drying at 100 °C in an oven until a constant weight was attained (m_2). In this way, the SD and gel fraction (GF) were calculated at a determined time according to eqn (1) and (2), respectively. Measurements were repeated in triplicates to acquire an average value.

$$\mathrm{SD}(\%) = \frac{(m_1 - m_o)}{m_o} \times 100 \quad (1)$$

$$\text{Gel yield}(\%) = \frac{m_2}{m_o} \times 100 \quad (2)$$

Mechanical properties. Tensile strength (TS) and elongation at break (EB) of the photo-crosslinked films were examined using Santam Universal Testing Machine, model SMT-20 (Iran) based on ASTM D-882. Longitudinal measurements of 10 points of three specimens for each sample were performed using Vernier calipers and the average thickness, width and length were 1, 20, and 100 mm, respectively. Film strips placed and clamped between extension tensile grips of the testing machine were stretched uniaxially with a crosshead speed of 5 mm min^{-1} until breaking (load range: 500 N).

Differential scanning calorimetric (DSC). T_g of the GelMA hydrogels was measured *via* a Mettler Toledo DSC (Module DSC 822e, Mettler-Toledo GmbH, Switzerland) (ASTM D3418-15). 5 mg of dried sample was loaded into a 10 μL aluminium pan hermetically sealed. The following heat-cool-reheat program was run for all samples under a nitrogen atmosphere: equilibration at 25 °C, heating from 25 to 120 °C (rate: 10 °C min^{-1}); cooling from 120 to 25 °C (rate: −10 °C min^{-1}), reheating to 120 °C (rate: 5 °C min^{-1}), and finally cooling down to 25 °C. Glass transition temperature (T_g) of each sample was found as the mid-point between onset and endset of the inflectional tangent of the second heating run.

Thermogravimetric analysis (TGA). Thermal stability of the pure gelatin and photo-crosslinked GelMA hydrogels was assessed using Perkin Elmer Pyris Dimond model TGA (USA) by measuring the weight of the sample as a function of temperature (ASTM E1131). 5 mg of each sample was heated at a heating rate of 10 °C min^{-1} in a temperature range of 20–600 °C under nitrogen atmosphere (N_2 flow: 50 cm^3 min^{-1}), and TGA data were achieved.

Water contact angle (WCA). The surface hydrophilicity of the photo-crosslinked GelMA films was evaluated *via* a water contact angle (WCA) measurement through the insertion of a 1.5 μL DI water droplet with a precision syringe on the surface (ASTM D7490-13). The shape of the sessile water droplets was captured by a Canon camera at 3 and 20 s after positioning. Then, WCA measurement was conducted according to the image processing by ImageJ software and DropSnake curve fitting of drop profile (Plugins/Drop_analysis/DropSnake), as the tangent of the baseline and the drop boundary. Five replicates were done on films and the average WCA values were recorded.

Molecular dynamics simulation (MDS). The BIOVIA Material Studio 2017 software (2017.1.0.48, Accelrys Inc., USA) was run to simulate the molecular structures and calculate the total energy to estimate the dipole moment (μ) of GMA and MA as their quantum properties. First, 3D molecular structures of GMA and MA were drawn in the 3D atomistic media of Material Studio. To optimize the molecular structure geometrically, Forcite geometry optimization was accomplished (module: Forcite/task: geometry optimization/forcefield: condensed-phase optimized molecular potentials for atomistic simulation studies (COMPASS)/Quality: Ultra-fine). All of the possible molecule conformers and their total energy were identified by Conformer Modules (task: Conformer Calculation/Forcefield: COMPASS) in the 3D Conformers Calculation list. Next, the μ of all of these possible conformers was specifically calculated and the average values were reported to study the interaction between the molecules and the MW radiation.

Results and discussion

As mentioned previously, the functional group-containing amino acids of gelatin such as LY, HLY, phenylalanine, methionine, serine, threonine, tyrosine, aspartic acid, and glutamic acid can be modified toward the particular purpose.[2,6,17,19,21] In this study, the preparation of GelMAs *via* the reaction of amine groups of LY and HLY with methacrylation reagents namely GMA and MA under both MW and conventional conditions was conducted and their products were compared to each other by using several evaluation methods.

Characterization

Fig. 2 illustrates the nucleophilic reaction mechanisms of amine groups existing on the gelatin chains with the epoxide

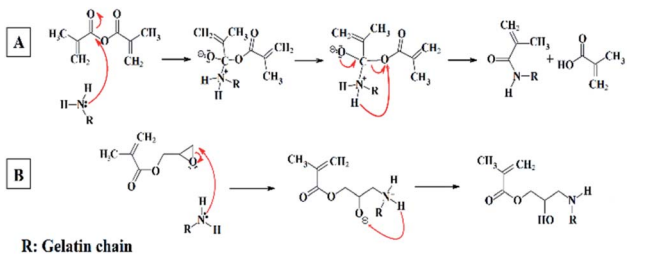

Fig. 2 The reaction mechanism of the amine group on gelatin with (A) MA and (B) GMA.

group of GMA and anhydride group of MA. According to Fig. 2, the coupling of MA with amine group results in methacrylamide bond formation, while (3-amino-2 hydroxy) propyl methacrylate group forms in the reaction of epoxide of GMA and amine group. The conjugation of methacryloyl groups through the reaction of gelatin with either GMA or MA was confirmed and quantified *via* ^{1}H NMR spectroscopy. ^{1}H NMR spectra of non-methacrylated gelatin, MW-G-5-5-500, MW-G-10-1-500, MW-M-10-1-500, C-G-5, C-G-10, C-M-5, and C-M-10 were outlined in Fig. 3. The intensity of the protons in all of the ^{1}H NMR spectra was normalized against the reference normalizing signal at δ 7.00–7.50 ppm centered at 7.40 ppm corresponds to the aromatic protons of phenylalanine amino acids which are chemically passive in the methacrylation reaction of gelatin and remain intact.[19,21,37] The appearance of characteristic resonance peaks of the two methylene protons of the methacrylate vinyl group (H_2C=C–) at around 5.40–5.80 and 5.95–6.30 ppm (2H) and methyl protons of the methacrylate vinyl group (C=C–CH_3) at around 1.80–2.20 ppm (3H) confirmed the methacrylation. It is obvious that the methylene protons (H_2C=C–) of GMA–GelMAs shifted to higher ppm compared to that of MA–GelMAs. Additionally, the intensity of the peaks at around 3.70 ppm which corresponds to the methylene proton adjacent to the hydroxyl group (–CH_2–OH) became more intensive in GMA–GelMAs rather than MA–GelMA, as a result of the epoxide ring-opening reaction. These peaks gradually increased with increasing GMA concentration. All of these peaks confirmed that GMA and MA were successfully grafted to the gelatin chains. Furthermore, since only LY and HLY amino acids possess the primary amines as reactive sites that can bound to GMA and MA *via* a nucleophilic addition reaction, a gradual decrease of methylene protons of LY and HLY signal (N–CH_2–C) at around 2.90 ppm (2H) can be considered to prove the GelMA synthesis. The extent of gelatin functionalization or MD was quantified by eqn (3) as the ratio of the integrated signals of LY and HLY methylene protons appeared at around 2.83–3.00 centered at 2.90 ppm in the GelMAs to that of the pure gelatin. These MD values were reported in Table 1. It is noteworthy to point that type A gelatin was used for GelMA synthesis in this study due to the higher amount of reactive primary amino groups than that of type B gelatin which can lead to a greater methacryloyl functionality.[21,37]

$$\mathrm{MD}(\%) = \left[1 - \frac{\text{protons peak area of LY and HLY methylene GelMA}}{\text{protons peak area of LY and HLY methylene gelatin}}\right] \times 100 \quad (3)$$

As shown in Fig. 3, the peak of LY and HLY methylene protons around 2.90–3.00 ppm disappeared in MW-G-5-5-500 spectra and its MD was calculated to be 96.1%, exhibiting a high level of methacryloyl substitution.

Fig. 4 displays the FT-IR spectra for gelatin, MW-G-5-5-500, MW-G-10-1-500, MW-M-10-1-500, C-G-5, C-G-10, C-M-5 and C-M-10. Pure gelatin and different GelMAs present the strong amide I absorption peak (C=O stretching) around 1630–1670 centered at 1639 cm^{-1}, amide II peak (C–N–C=O symmetry stretching and N–H in-plane bending) around 1500–1580 centered at 1512 cm^{-1}, amide III peak (C–N stretching) at around 1220–1250 centered at 1234 cm^{-1} and amide A peak (N–H and O–H stretching) as a prominent broad spike around 3200–3600 centered at 3420 cm^{-1}.[19,21,36]

Generally, the presence of methacrylate vinyl group can be traceable by C=C stretching absorption peak at 1630–1680

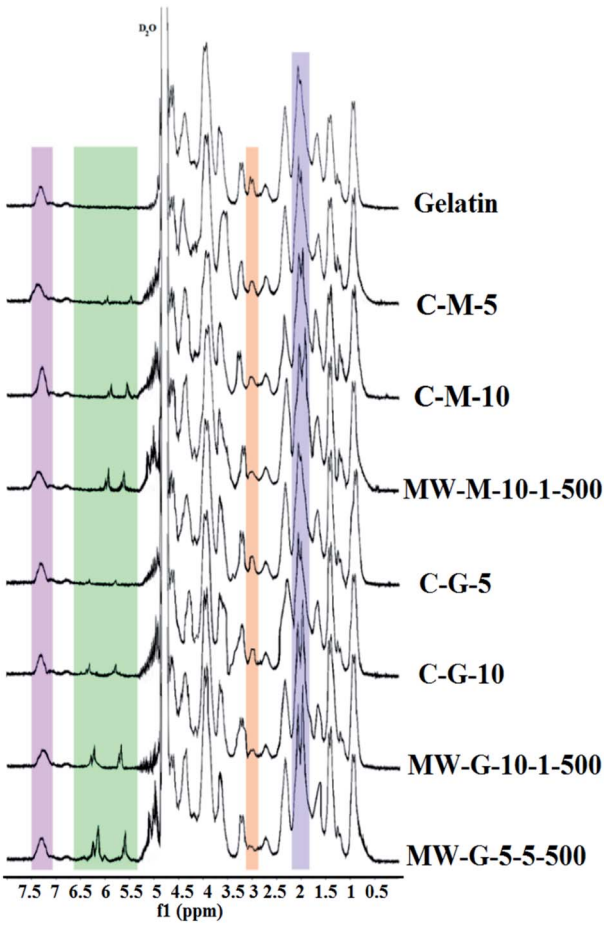

Fig. 3 ^{1}H NMR spectra representative for gelatin, MW-G-5-5-500, MW-G-10-1-500, MW-M-10-1-500, C-G-5, C-G-10, C-M-5 and C-M-10.

Table 1 MD values of different GelMAs using ^{1}H NMR calculation

GelMA	MD%
MW-G-5-5-500	96.1
MW-G-10-1-500	89.1
MW-M-10-1-500	77.5
C-M-10	65.3
C-M-5	51.9
C-G-10	45.2
C-G-5	36.4

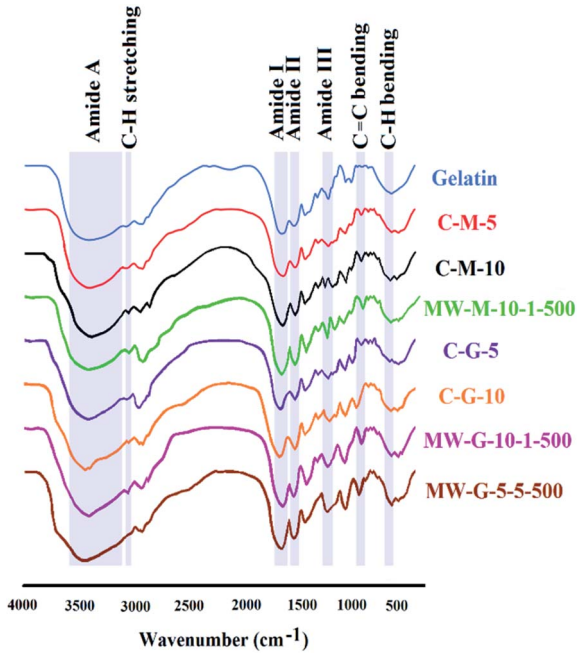

Fig. 4 FT-IR spectra for gelatin, MW-G-5-5-500, MW-G-10-1-500, MW-M-10-1-500, C-G-5, C-G-10, C-M-5 and C-M-10.

centered at 1640 cm^{-1}, but this peak was concealed by the strong amide I signal in the GelMAs.[3,19,21] However, the appeared C=C bending absorption peak in GelMAs around 940–970 cm^{-1} centered at 950 cm^{-1} confirm the methacrylation reaction *via* the MWA and conventional methods using both GMA and MA. It was observed that the intensity of amide I, II and III peaks in MA–GelMAs increased compared to pure gelatin (MW-M-10-1-500 > C-M-10 > C-M-5) which can be attributed to the amide-bond formation and incorporation of C=O group of methacrylate in the GelMA structure according to Fig. 2.

Also, the intensity of amide I and III peaks increased in GMA–GelMAs (MW-G-5-5-500 > MW-G-10-1-500 > C-G-10 > C-G-5) compared to gelatin due to the overlap with C=O stretching of attached methacrylate group and overlap with the hydroxyl group formed, respectively. In other words, as a result of ring-opening reaction of epoxide and primary amines, –OH stretching peak of GMA–GelMAs can be detected at 1238 cm^{-1} but it was concealed by amide III that appeared in 1220–1250. So, increasing the intensity of amid I and III in GMA–GelMAs confirmed the methacryloyl conjugation. Besides, amide A peak corresponding to the N–H and O–H stretching was broadened and left-shifted in C-G-5, C-G-10, MW-G-10-1-500 and MW-G-5-5-500 due to the hydroxyl group formation. MW-G-5-5-500 has the widest amide A peak among the GelMAs. Nevertheless, the methacrylation leads to the spectral changes including increasing the amide I, II, III intensity, broadening of the vibration assigned to simultaneous O–H and N–H stretches, and also a slight left shift of amide A spike from 3420 to 3480 cm^{-1} that is not significant. The characteristic absorption bands of saturated C–H stretching for $-CH_3$ and $-CH_2-$ around 3050–3100 centered at 3083 cm^{-1} appeared in all of the GelMAs. Strong absorption peaks of saturated C–H bending around 670–730 cm^{-1} were shown in Fig. 4, as well. It is obvious that the intensity of C–H stretching and bending increased by MD increment. In addition, $C{=}C{-}H_2$ wagging and =C–H bending vibrations appeared at 672 cm^{-1} in all GelMAs. Only some minor differences could be observed in the rest of the spectra. A comparison between the absorption peak of C=C bending signified that the content of C=C expectedly increased with the increase of MD.

Raman scattering method as vibrational molecular spectroscopy arises from an inelastic light scattering procedure.[37,38] Functional groups of pure gelatin and MW-G-5-5-500 were identified by using Raman spectroscopy and are represented in Fig. 5. It was found that there are nearly similar bands between 400 and 3500 cm^{-1} in both FT-IR and Raman spectra. The characteristic peaks identified in Raman spectra of gelatin and MW-G-5-5-500 include weak O–H and N–H stretching peaks around 3200–3600 centered at 3250 cm^{-1}, intense C–H stretching peaks around 2800–3000 centered at 2950 cm^{-1},

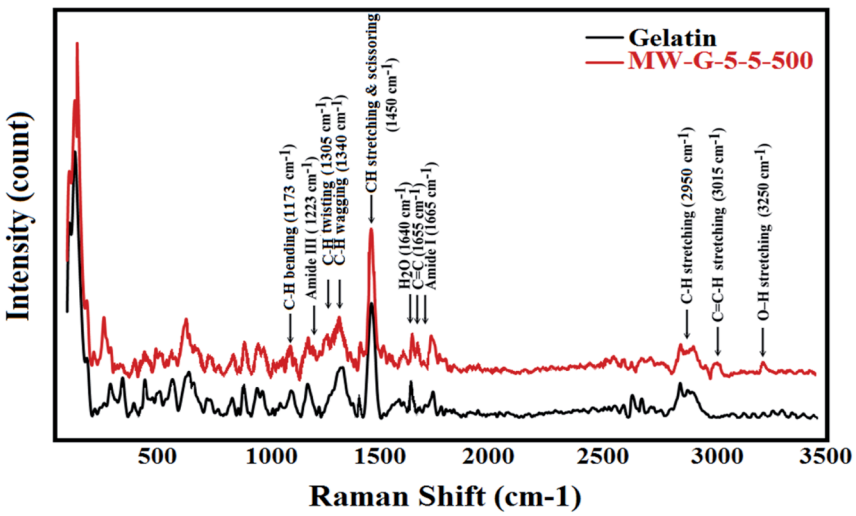

Fig. 5 Raman spectra for pure gelatin and MW-G-5-5-500.

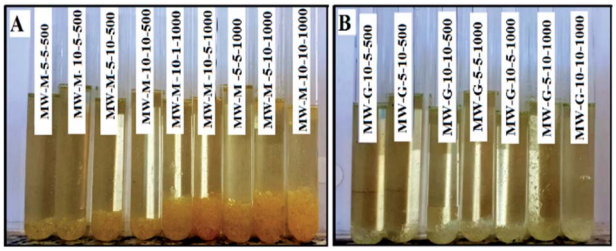

Fig. 6 Two-phase GelMA solutions obtained by the MWA method (A: MA–GelMAs and B: GMA–GelMAs solutions).

weak C=O stretching (amide I) at 1665 cm^{-1}, weak NH bending at 1613 cm^{-1}, C=C of tyrosine at 1615–1618 cm^{-1}, strong CH stretching and scissoring (methyl (CH_3) and methylene (CH_2)) around 1420–1470 centered at 1450 cm^{-1}, strong CH wagging at 1335–1343 cm^{-1}, strong CH twisting at 1300–1315 cm^{-1}, amide III (C–N stretching) at 1223 cm^{-1}, C–H bending at 1173 cm^{-1}, C–N stretching in proline at 1127–1150 cm^{-1}, C–C skeletal in backbone at 1064–1080 cm^{-1}, symmetric ring breathing of phenylalanine at 1003–1030 cm^{-1}, C–H in-plane bending at 1031 cm^{-1}, phenylalanine at 620 cm^{-1} and N–H bending at 599 cm^{-1}. Also, a weak peak around 1640 cm^{-1} is correlated to H_2O. There are some peaks in Raman spectrum of MW-G-5-5-500 which confirmed the methacrylation: C=C stretching at 1655 cm^{-1}, medium C=C–H stretching peak around 3000–3100 centered at 3015 cm^{-1}, and medium O–H stretching peak centered at 3250 cm^{-1} corresponding to the hydroxyl group resulted from the ring-opened epoxide group. Additionally, the peaks corresponded to the CH_2 and CH_3 at 1450 cm^{-1} are more intensive in MW-G-5-5-500 confirming the methacrylation.[37,38]

The effect of methacrylation reagents and methods

As mentioned in Tables S1 and S2,† the reactivity comparison of the methacrylation reagents (GMA and MA) with gelatin under the MW and conventional conditions has been carried out.

As shown in Fig. 6 and Table S1,† some of the MWA synthesized GelMA solutions prepared under the high MW power (500 and 1000 W) and long reaction times (5 and 10 min) having a high GMA or MA concentration (*i.e.* MW-G-5-5-1000, MW-G-5-10-500, MW-G-5-10-1000, MW-G-10-5-500, MW-G-10-5-1000, MW-G-10-10-500, MW-G-10-10-1000, MW-M-5-5-500, MW-M-5-5-1000, MW-M-5-10-500, MW-M-5-10-1000, MW-M-10-1-1000, MW-M-10-5-500, MW-M-10-5-1000, MW-M-10-10-500 and MW-M-10-10-1000) were phase-separated while all of the GelMA solutions prepared by the conventional method were one-phase and homogenous. Consequently, it can be understood that in the MWA method prolonging the irradiation time at high MW power does not yield homogenous products, especially in the presence of a high amount of GMA or MA. Also, it is obvious in Fig. 6 that precipitation behaviour is more severe in the MA–GelMA solutions synthesized by the MWA method. Moreover, it can be found that the amount of separated phase increased by increasing the GMA or MA concentration, irradiation time, and MW power. The pH values of the synthesized GelMA solutions were reported in Table 2. According to these results, the MWA methacrylation reaction of gelatin using MA led to acidic media (pH: 5.5–6.1) while pH values of the MWA

Table 2 Characteristics of the photo-cured GelMA hydrogel films

No.	Code	pH	Hydrogel condition	GF (%)	SD (%)	T_g (°C)	TS (MPa)	EB (%)
1	MW-G-5-1-100	7.1	Weak hydrogel	22	NA[a]	NA	NA	NA
2	MW-G-5-1-500	7	Ok	82.7	25.8	64.11	5.05	114.7
3	MW-G-5-1-1000	7.3	Ok	93	14.71	70.20	6.62	152.4
4	MW-G-5-5-100	7.2	Ok	37.2	45	58.32	3.23	32.7
5	MW-G-5-5-500	7	Ok	98.3	10.11	75.34	6.7	175.2
6	MW-G-5-10-100	7.4	Ok	63.6	36.31	59.85	4.01	79.5
7	MW-G-10-1-100	7.3	Weak hydrogel	24.1	NA	NA	NA	NA
8	MW-G-10-1-500	7.5	Ok	92.5	18.41	71.58	5.55	129.9
9	MW-G-10-1-1000	7.4	Ok	94.2	11.4	71.81	6.61	163.6
10	MW-G-10-5-100	7.2	Weak hydrogel	25.3	NA	NA	NA	NA
11	MW-G-10-10-100	7.4	Ok	74	29.91	64.48	4.4	93.2
12	MW-M-5-1-100	6.1	Weak hydrogel	17.2	NA	NA	NA	NA
13	MW-M-5-1-500	5.9	Weak hydrogel	18.4	NA	NA	NA	NA
14	MW-M-5-1-1000	5.5	Weak hydrogel	23	NA	NA	NA	NA
15	MW-M-5-5-100	5.9	Weak hydrogel	19	NA	NA	NA	NA
16	MW-M-5-10-100	5.9	Ok	61	44.71	59.53	3.73	62.4
17	MW-M-10-1-100	6	Weak hydrogel	17.5	NA	NA	NA	NA
18	MW-M-10-1-500	5.7	Ok	79.3	23.81	67.46	5.2	122.8
19	MW-M-10-5-100	6	Weak hydrogel	20.7	NA	NA	NA	NA
20	MW-M-10-10-100	6.1	Ok	68	32.71	64.32	4.24	85
21	C-G-5	7.2	Ok	28	70.1	58.27	2.5	24.1
22	C-G-10	7.3	Ok	63.4	41.51	60.18	3.86	51.8
23	C-M-5	7.2	Ok	62.3	59.71	62.19	3.72	49
24	C-M-10	7	Ok	75.3	27.11	64.80	4.41	98.6

[a] Not applicable.

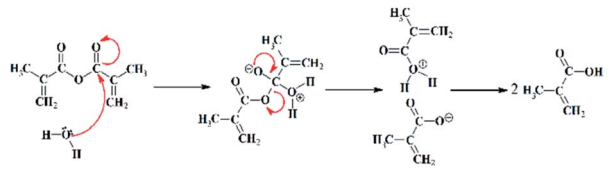

Fig. 7 MA hydrolysis mechanism in aqueous media.

synthesized GelMA solutions attained by GMA were neutral (pH: 7–7.5). Also, GMA– or MA–GelMA solutions achieved by the conventional method had a neutral pH. Since the methacrylation reactions take place in an aqueous environment, MA will be hydrolysed and decomposed into two methacrylic acids which can drop pH and be homopolymerized under the MW condition. The mechanism of MA hydrolysis is revealed in Fig. 7.

The precipitated phase of MW-M-10-10-1000 and MW-G-10-10-1000 were separated, dried in an oven at 100 °C for 24 h, and analysed by DSC to achieve their T_g values. As can be seen in Fig. 8, T_g values of the precipitated phase of MW-G-10-10-1000 and MW-M-10-10-1000 were found to be 59.30 °C and 219.90 °C, respectively. These T_g values are almost equal to the T_g of GMA homopolymer (~61 °C) and methacrylic acid homopolymer (~228 °C), respectively. Therefore, this phenomenon can be associated with the probable homopolymerization of GMA and methacrylic acid or even MA monomers in some of the methacrylation reaction conditions, at high MW power and monomer concentration as well as long reaction times.

In the following, only one-phase GelMA solutions were considered to be photo-crosslinked and two-phase products were discarded.

Photo-crosslinking under visible light with a non-cytotoxic and biocompatible photoinitiator, VA-086, was accomplished due to the limited penetration depth of UV irradiation and its detrimental influence on the alive cells.[44–49] Furthermore, GelMA and VA-086 concentrations were selected according to the optimum values reported in previous studies.[45–49] GelMA is not capable of being thoroughly dissolved in water above 15% (w/v).[32,37] Besides, it has been proven that VA-086 with a concentration below 1.5% (w/v) has generally non-cytotoxic behavior.[46–49] Hence, GelMAs obtained from one-phase solutions were dissolved in DW (15% (w/v)) and subsequently LED-cured *via* free-radical polymerization in the presence of 1% (w/v) of VA-086. During the light exposure, VA-086 absorbs photons and dissociates into free radicals that will propagate through the methacrylate groups and form the covalent bonds between GelMA chains.[47,49] In this study, the concentration of GelMAs and VA-086, as well as irradiation dose were selected to be constant in all of the experiments.

The results of the SD after 2 min and GF after 48 h extraction in water were presented in Table 2. As can be seen in Table 2, GF and SD of synthesized hydrogels were found to be in the range of 17–99% and 10–70%, respectively. Pure gelatin has a GF of about 20%. Generally, hydrogels having GF values below 25% did not have standing films and were categorized as weak hydrogels in Table 2, namely MW-M-10-1-100, MW-M-5-5-100, MW-M-10-5-100, MW-M-5-1-1000, MW-M-5-1-500, MW-M-5-1-100, MW-G-10-5-100, MW-G-10-1-100 and MW-G-5-1-100. However, the other GelMA hydrogels achieved by the MWA method were found to be relatively strong and had higher GF compared to the GelMA hydrogels obtained by the conventional method. In other words, the synthesized GelMAs by using both GMA and MA under the MW irradiation had higher MD (77.5–96.1%) rather than that obtained by the conventional method (36.4–65.3%), according to Table 1.

Considering the results of ^{1}H NMR, FT-IR and Raman spectroscopic analyses and MDs in Table 1, it can be concluded that approximately all of the primary amine groups were consumed after 5 min irradiation under MW for MW-G-5-5-500 while the amine groups in C-G-5 and C-G-10 remained almost constant and only a minor portion of that reacted. So, it seems that highly methacrylated gelatin and strong hydrogels can be attained by applying the optimized process parameters in the MWA method.

The effect of methacrylation reagent in the MWA method can be evaluated by the comparison between samples such as MW-G-5-1-100 and MW-M-5-1-100, MW-G-10-1-100 and MW-M-10-1-100, *etc.* According to Table 2, the comparison between GF, SD, TS, EB, and T_g of the abovementioned hydrogels reveals that GMA has higher efficiency and better performance to functionalize the gelatin rather than MA under the MW irradiation in the same MW power, concentration, and reaction time. Also, Table 1 shows that the extent of MD in MW-G-10-1-500 is about 89.1%, whilst the MD of MW-M-10-1-500 is about 77.5%. Consequently, in the same condition under the MW irradiation

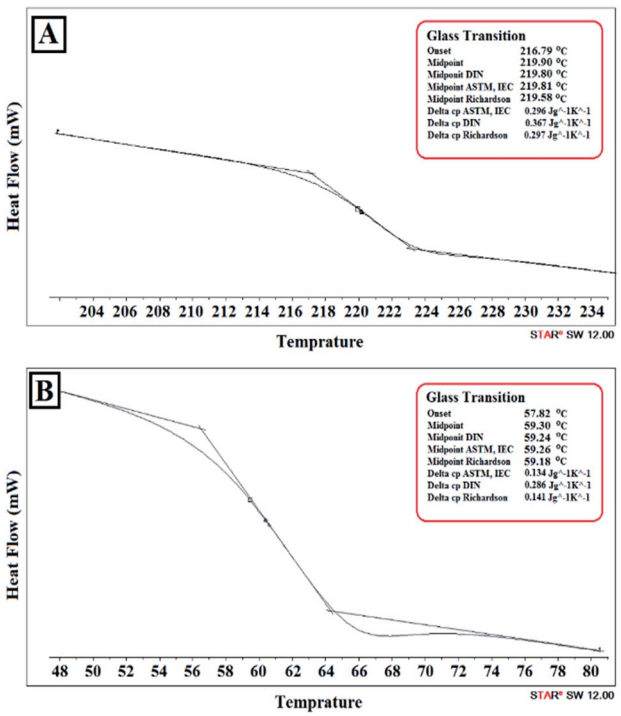

Fig. 8 DSC thermograph of the precipitated phase in (A) MW-M-10-10-1000 and (B) MW-G-10-10-1000.

(reagent concentration: 10, reaction time: 1 min, MW power: 500), MW-G-10-1-500 has higher MD compared to the MW-M-10-1-500. Higher TS, EB, GF, and T_g of the photo-crosslinked GelMA hydrogels attained by GMA over MA in the same synthesis condition is undoubtedly attributed to the higher jointing probability of photo-sensitive groups grafted to gelatin chains. To justify the better performance of GMA in comparison to MA under the MW condition, their electronic structure should be considered. In response to the oscillating electric field of MW as electromagnetic waves, only dipolar (permanent or induced dipoles) and ionic substances can selectively absorb MW energy, be aligned frequently, and generate heat. This frequent reorientation leads to the strong rotation, movement, agitation, collisions, and friction between species.[39–43] Subsequently, the supremacy of the MWA method can be described comprehensively by the dielectric properties and relaxation time of the reactants and solvents.[39–43] Dielectric constant (ε_r) is a vital quantity to estimate and compute the reactivity of materials under the MW conditions.[40–42] According to the SS1 section and eqn (S1) mentioned in the ESI,† ε_r can be calculated by using the dipole moment (μ) as an electronic descriptor which commonly describes the polarity of components and the distribution of the electrons on the molecules.[50–53] Generally, molecules with large μ have higher electronic interactions with other molecules, more spatial molecular conformers, and a higher tendency to be excited rotationally in the presence of the MW field, leading to better performance in chemical reactions.[53–56]

The μ values of GMA and MA were generated by Material Studio to examine their reactivity in the MWA reaction based on the SS2–SS4 procedures and Fig. S5–S10† mentioned in the ESI. The geometry optimized molecular structures and averaged μ values of GMA and MA are depicted in Fig. 9. The achieved μ values of GMA and MA are 3.675 ± 0.036 and 3.256 ± 0.042 (Debye), respectively. Therefore, the superior performance of GMA compared to MA in the MWA methacrylation reaction of gelatin can be justified according to its higher μ value which exhibits higher electronic interactions.[50,53,57–61]

In contrast, based on the results mentioned in Tables 1 and 2, C-M-5 and C-M-10 had higher MD, GF, SD, T_g, TS, and EB compared to the C-G-5 and C-G-10, respectively. Hence, in the conventional conditions, MA has higher efficiency rather than GMA. This conclusion is in good agreement with the results have already reported by other researchers.[3,19,21,27]

Worth mentioning that GMA–GelMA with an MD of 96.1% can be obtained by MW irradiation in 5 min, while MD of MA–GelMA reached 77.5% after a 4 h reaction in the conventional method. Therefore, the superiority of the MWA method in comparison to the conventional method for achieving high MD in a short time is obvious.

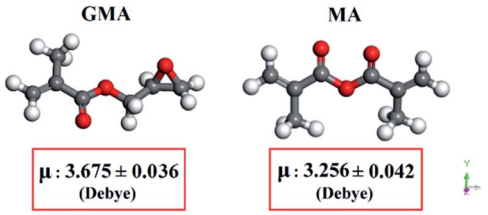

Fig. 9 Geometry optimized molecular structure and the averaged μ of MA and GMA.

The effect of GMA and MA concentration in the MWA method

The comparison between GMA–GelMAs such as MW-G-5-1-100 and MW-G-10-1-100 reveals that doubling the GMA concentration from 5 times to 10 times under the same MW irradiation condition resulted in the hydrogels with higher GF, TS, EB, and T_g. Also, doubling the MA concentration from 5 times to 10 times under the same MW irradiation led to the MA–GelMA hydrogels with higher GF, TS, EB, and T_g values such as MW-M-5-1-100 and MW-M-10-1-100. Consequently, the increase of GMA or MA concentration under the constant MW power and reaction time results in greater GF values, confirming the significant role of GMA and MA concentration in the methacrylation reactions. It is noteworthy that increasing the GMA or MA concentration in some cases led to the two-phase products, *e.g.*, MW-G-5-5-1000 to MW-G-10-5-1000 and MW-M-5-1-1000 to MW-M-10-1-1000, as highlighted in Fig. 6 and Table S1.†

The effect of irradiation time in the MWA method

The results reported in Table S1† show that by increasing the irradiation time from 1 to 5 and 10 or 5 to 10 min the GF values increased, for example in MW-G-5-1-100 (22%) and MW-G-5-5-100 (37.2%) or MW-G-10-5-100 (25.3%) and MW-G-10-10-100 (74%). It was expressed previously that increasing the reaction time in some GelMA synthesizes by GMA and MA resulted in two-phase products as can be seen in Fig. 6 and Table S1.†

The effect of MW power in the MWA methacrylation

As can be seen in Table S1,† the increasing of the MW power in one-phase GMA and MA-prepared GelMA solutions resulted in the hydrogels with greater GF, TS, EB, and T_g values. For instance, by 5 or 10 multiplying the MW power, the GF value of MW-G-5-1-100 increased from 22% to 82.7% (MW-G-5-1-500) and 93% (MW-G-5-1-1000) or the GF value of MW-M-10-1-100 increased from 17.5% to 79.3% (MW-M-10-1-500). It should be noticed that in some cases, increasing the MW power led to the two-phase GelMA solutions (see Table S1† and Fig. 6).

The effect of MD on mechanical, thermal, and surface properties of GelMA hydrogels

From the above discussion, the optimum GelMA synthesis condition is associated with the MW-G-5-5-500 (methacrylation method: MWA, methacrylation reagent: GMA, irradiation time: 5 min, reagent concentration: 5 times molar excess of GMA over the primary amines, MW power: 500 W). In the following, the relation between MD of GelMAs and mechanical, thermal, and surface properties of the hydrogels will be investigated.

Generally, the GF values quantify the photo-crosslinking success to provide the covalent bonds between chains in the 3D network, while SD indicates the amount of migration and

leaching out of the polymer chains that were not joined together from the network into the water by diffusion.[17,22,25]

The results in Tables 1 and 2 reveals that the GF values increase from 28% to 98.3% by increasing the MD from 36.4% to 96.1% due to the higher crosslinking density. Thus, by increasing the MD, GF values increase and SD values decrease. So, the GF values are opposite to the SD results. Moreover, the maximum and minimum MD and GF were achieved for MW-G-5-5-500 and C-G-5, respectively, among all the samples.

Tensile mechanical properties of the GelMA hydrogels, *i.e.* TS and EB are listed in Table 2 and illustrated in Fig. 10 and S11 (see ESI section†). TS and EB of the pure gelatin films were expressed to be approximately 3 MPa and 5%, respectively. The comparison between TS, EB, T_g, and GF of the GelMA hydrogels are outlined in Fig. 10. The highest mechanical properties belonged to MW-G-5-5-500 with TS and EB of 6.7 MPa and 175.2%, respectively. It can be seen in Fig. 10 that TS, EB, and T_g of the photo-crosslinked GelMAs increased by GF increments suggesting better covalent crosslinking. Therefore, it can be concluded that TS and EB of the hydrogels can be tuned by changes in MD and GF values.

The T_g values of the pure gelatin and photo-crosslinked GelMAs were determined from DSC thermograms and presented in Table 2 and Fig. 10. After irradiation, T_g increased significantly from 58 °C for gelatin to a range of 61–75 °C, due to the new covalent bonds formed in the gelatin network which limit the mobility of chain segments and act as inelastic nodes, leading to the higher T_g values. Also, changes in the local molecular packing and decreasing the free volume are the results of crosslinking. This was examined by other researchers that the properties of the GelMA hydrogels can be eagerly tailored by changing the MD, photoinitiator and GelMA concentration, as well as intensity and irradiation time (irradiation dose).[21–26,28–34]

The relation between MD and GF, SD, EB, TS, and T_g of photo-crosslinked GelMA hydrogels are shown in Fig. 11 (solid lines) and the equation of best curve fitting for each data was derived (dotted lines) as follows:

$$(GF = 0.001\ MD^3 - 0.2052\ MD^2 + 14.734\ MD - 280.53,\ R^2 = 0.967),$$

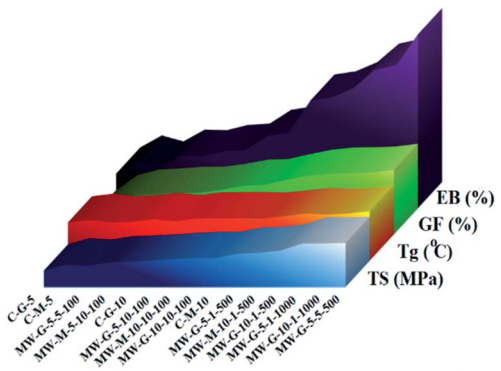

Fig. 10 Comparison between TS, EB, T_g, and GF of LED-cured GelMA hydrogels.

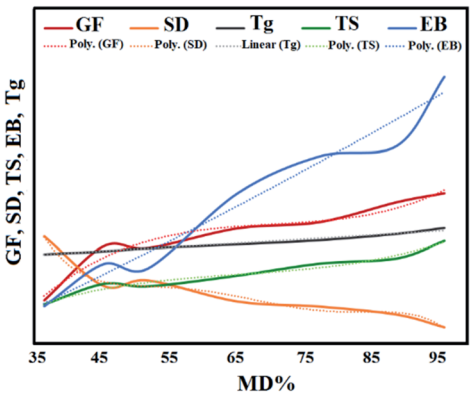

Fig. 11 Relation between MD and GF, SD, EB, TS, and T_g of LED-cured GelMA hydrogels.

$$(SD = -0.000002\ MD^5 + 0.0008\ MD^4 - 0.1079\ MD^3 + 7.0756\ MD^2 - 227.84\ MD + 2928.4,\ R^2 = 0.9818),$$

$$(EB = 0.0034\ MD^2 + 1.8762\ MD - 47.02,\ R^2 = 0.962),$$

$$(TS = 0.0004\ MD^3 - 0.0802\ MD^2 + 5.5642\ MD - 90.063,\ R^2 = 0.972),$$

$$(T_g = 0.2698\ MD + 47.898,\ R^2 = 0.9776).$$

The objective of measuring the static WCAs was to compare the wettability of the photo-crosslinked GelMA films. It was observed that water droplets didn't reach the equilibrium state on these hydrophilic gelatin-based surfaces due to the fairly fast substrate water absorption. Thus, left (L) and right (R) WCAs at 3 and 20 s were measured and reported as a metastable equilibrium in Fig. 12. According to Fig. 12, pure gelatin exhibits a hydrophilic surface with a small WCA of 55°, but the WCA of GelMA films increased to the range of 57° to 72° after irradiation. It is worthy to state that WCAs of the GelMA films reduced from the range of 57–72° at 3 s to 50–68° at 20 s. So, all of the surfaces possess hydrophilic behavior that their WCAs tend to slightly decrease down after a while. Based on Fig. 12, MW-G-5-5-500 and C-G-5 have the highest (72°) and the lowest (57°) WCAs, respectively. The high WCA of MW-G-5-5-500 might be associated with the high MD and high crosslinking density in the cured film. According to Fig. 2, the methacrylated functionality length obtained from GMA is longer than that of MA; subsequently, GMA-methacrylated functionality can easily rotate and is more accessible in the photo-crosslinking reactions to join the GelMA chains and make them stiffer. The comparison of WCAs of MW-G-5-10-100 (64.02°) and MW-M-5-10-100 (63.1°) or MW-G-10-1-500 (69.59°) and MW-M-10-1-500 (68.57°) indicates that the hydroxyl groups produced by the ring-opening reaction of epoxide and amine groups do not increase the hydrophilicity of the surface. Consequently, the MD or GF is more impressive than the hydrophilic hydroxyl groups on the hydrogel surface hydrophilicity. Hence, the high WCA of MW-G-5-5-500 can be justified by its high MD and GF

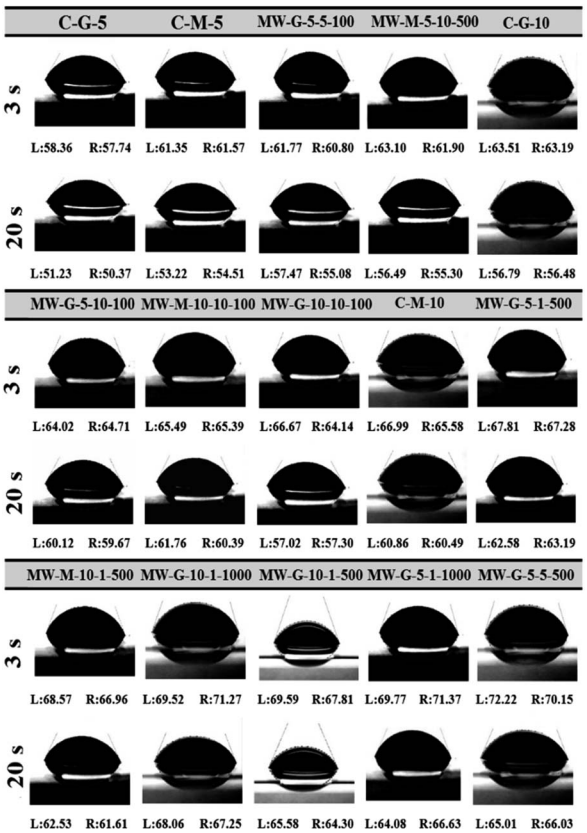

Fig. 12 Left and right WCA of LED-cured GelMA hydrogels.

values. Furthermore, WCA results are in agreement with the GF, SD, TS, EB, and T_g results.

TGA thermograms of pure gelatin and MW-G-5-5-500 are shown in Fig. 13. As can be seen, both of them display multiple weight loss zones, associated with the evaporation and decomposition of their components. The first shoulder of both specimens was around 90–95 °C which corresponds to the water evaporation. The temperature of this stage was not significantly different for pure gelatin and MW-G-5-5-500, but the weight loss fraction at this stage was dissimilar because of the different moisture contents of these hydrogels. The major weight loss of gelatin and MW-G-5-5-500 relates to the degradation of chains (helical protein chain breakage and peptide bonds rupture) started at about 270 °C and 280 °C, respectively. Also, it is detected that the weight loss rates of gelatin and MW-G-5-5-500 are maximum at 290–380 °C and 300–400 °C, peaking at 310 °C and 320 °C, respectively. Therefore, it is understandable that the weight loss rate of MW-G-5-5-500 is lower compared to that of pure gelatin. This result proposes that higher thermal stability is provided by the covalent crosslinking between protein chains.

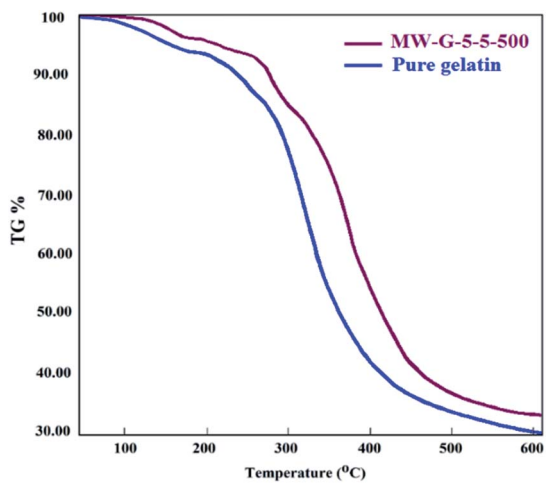

Fig. 13 TGA thermograph of pure gelatin and MW-G-5-5-500.

Besides, there is no weight loss shoulder in the TGA thermograph of MW-G-5-5-500 around 189 °C corresponding to the boiling point of GMA. This illustrates that the 1 day purification of MWA-synthesized GelMA guarantees sufficient purity. Therefore, less amount of methacrylation reagents and higher reaction speed under the MW circumstances reduced the sufficient purification time compared to the conventional method which needs more than 2 weeks purification. According to the approved biocompatibility of GelMAs and VA-086 by several studies, being harmlessness of visible light irradiation on living cells, high MD of MW-G-5-5-500 which provides a suitable mechanical strength, and proper purification confirmed by TGA analysis, it can be claimed that synthesized GelMAs can be considered as a promising precursor for bioprinting and bio-coating applications *e.g.* tissue engineering and food packaging.

Conclusions

In this contribution, a green technique for the synthesis of a highly functionalized GelMA that can be stably LED-cured was introduced by using MW and GMA to overcome the deficiencies of the conventional method. Comparative investigations between the MWA and conventional methacrylation reactions in presence of GMA and MA were performed comprehensively. The dependence of GF, SD, TS, EB, T_g, and WCA of the LED-cured GelMAs on the GMA and MA concentration, reaction time, and MW power was examined. The findings signified that GMA had the higher performance in the MWA method to methacrylate the gelatin in comparison to MA while in the conventional method MA acts better than GMA. Molecular dynamics simulation was considered to justify the superior performance of GMA compared to MA under the MW condition. It was concluded that increasing the GMA and MA concentrations, reaction time, and MW power to the optimum values enhanced GF, TS, EB, T_g, WCA, and MD of the hydrogels. Besides, the mathematical relations between MD and GF, SD, TS, EB, and T_g were provided. Finally, the optimized conditions to attain the highly methacrylated GelMA (MD: 96.1%) using GMA under MW conditions were introduced (5 min irradiation, power of 500 W, and 5 times molar excess of over the primary amine groups of gelatin). The suitable physical–mechanical properties of this photo-crosslinked hydrogel (GF: 98.3%, SD: 10.11%, TS: 6.7 MPa, and EB: 175.2%), and its good thermal property (T_g: 75.34 °C), and hydrophobicity (WCA: 72.22°)

suggested its applicability as bio-printing and bio-coating precursors.

Conflicts of interest

There are no conflicts to declare.

References

1 J. Zhu and R. E. Marchant, Design properties of hydrogel tissue-engineering scaffolds, *Expert Rev. Med. Devices*, 2011, **5**, 607–626.
2 J. Ma, Y. Wang and J. Liu, Bioprinting of 3D tissues/organs combined with microfluidics, *RSC Adv.*, 2018, **8**, 21712.
3 H. M. Enamul, N. Tamrin, Y. Tshai Kim, N. Norshariza and R. G. S. V. Prasad, Gelatin based scaffolds for tissue engineering – a review, *Polym. Res. J.*, 2015, **9**, 15–32.
4 Zh. Dong, Q. Yuan, K. Huang, W. Xu, G. Liu and Zh. Gu, Gelatin methacryloyl (GelMA)-based biomaterials for bone regeneration, *RSC Adv.*, 2019, **9**, 17737.
5 K. Goodarzi, F. Jonidi Shariatzadeh, A. Solouk, S. Akbari and H. Mirzadeh, Injectable drug loaded gelatin based scaffolds as minimally invasive approach for drug delivery system: CNC/PAMAM nanoparticles, *Eur. Polym. J.*, 2020, **139**, 109992.
6 R. Dash, M. Foston and A. J. Ragauskas, Improving the mechanical and thermal properties of gelatin hydrogels cross-linked by cellulose nanowhiskers, *Carbohydr. Polym.*, 2013, **91**(2), 638–645.
7 H. U. Zaman, M. A. Khan and R. A. Khan, Comparison of mechanical and degradation properties of EG and EGDMA grafted gelatin films, *J. Adhes. Sci. Technol.*, 2013, **27**(4), 413–422.
8 L. Solorio, C. Zwolinski, A. W. Lund, M. J. Farrell and J. P. Stegemann, Gelatin microspheres crosslinked with genipin for local delivery of growth factors, *J. Tissue Eng. Regener. Med.*, 2010, **4**(7), 514–523.
9 S. Sahraee, B. Ghanbarzadeh, J. M. Milani and H. Hamishehkar, Development of Gelatin Bionanocomposite Films Containing Chitin and ZnO Nanoparticles, *Food Bioprocess Technol.*, 2017, **10**, 1441–1453.
10 Q. Zhang, Ch. Qian, W. Xiao, H. Zhu, J. Guo, Z. Ge and W. Cui, Development of a visible light, cross-linked GelMA hydrogel containing decellularized human amniotic particles as a soft tissue replacement for oral mucosa repair, *RSC Adv.*, 2019, **9**, 18344.
11 R. Bhat and A. A. Karim, Towards producing novel fish gelatin films by combination treatments of ultraviolet radiation and sugars (ribose and lactose) as cross-linking agents, *J. Food Sci. Technol.*, 2014, **51**(7), 1326–1333.
12 I. V. Nieuwenhove, A. Salamon, K. Peters, G. J. Graulus, J. C. Martins, D. Frankel, K. Kersemans, F. De Vos, S. V. Vlierberghe and P. Dubruel, Gelatin- and starch-based hydrogels. Part A: hydrogel development, characterization and coating, *Carbohydr. Polym.*, 2016, **152**, 129–139.
13 Impact of electron beam irradiation on fish gelatin film properties, N. Benbettaie, Th. Karbowiak, C. H. Brachais and F. Debeaufort, *Food Chem.*, 2016, **195**, 11–18.
14 M. Bartnikowski, R. M. Wellard, M. Woodruff and T. Klein, Tailoring hydrogel viscoelasticity with physical and chemical crosslinking, *Polymers*, 2015, **7**, 2650–2669.
15 W. Du, Z. Zhang, W. Fan, W. Gao, H. Su and Zh. Li, Fabrication and evaluation of polydimethylsiloxane modified gelatin/silicone rubber asymmetric bilayer membrane with porous structure, *Mater. Des.*, 2018, **158**(15), 28–38.
16 J. W. Nichol, S. T. Koshy, H. Bae, C. M. Hwang, S. Yamanlar and A. Khademhosseini, Cell-laden microengineered gelatin methacrylate hydrogels, *Biomaterials*, 2010, **31**(21), 5536–5544.
17 S. Suvarnapathaki, M. A. Nguyen, X. Wu, S. P. Nukavarapu and G. Camci-Unal, Synthesis and characterization of photocrosslinkable hydrogels from bovine skin gelatin, *RSC Adv.*, 2019, **9**, 13016.
18 X. Li, Sh. Chen, J. Li, X. Wang, J. Zhang, N. Kawazoe and G. Chen, 3D culture of chondrocytes in gelatin hydrogels with different stiffness, *Polymers*, 2016, **8**, 269.
19 M. Sivakumar, P. Rajalingam Ganga Radharishman and H. Kothandaraman, Grafting of glycidyl methacrylate onto gelatin, *J. Appl. Polym. Sci.*, 1991, **43**, 1789–1794.
20 Ch. M. Elvin, T. Vuocolo, A. G. Brownlee, L. Sando, M. G. Huson, N. E. Liyou, P. R. Stockwell, R. E. Lyons, M. Kim, G. A. Edwards, G. Johnson, G. A. McFarland, J. A. M. Ramshaw and J. A. Werkmeister, A highly elastic tissue sealant based on photopolymerised gelatin, *Biomaterials*, 2010, **31**, 8323–8331.
21 K. Yue, G. Trujillo-de Santiago, M. Moises Alvarez Ali Tamayol, N. Annabi and A. Khademhosseini, Synthesis, properties, and biomedical applications of gelatin methacryloyl (GelMA) hydrogels, *Biomaterials*, 2015, **73**, 254–271.
22 Z. Wang, X. Jin, R. Dai, J. F. Holzman and K. Kim, An ultrafast hydrogel photocrosslinking method for direct laser bioprinting, *RSC Adv.*, 2016, **25**, 1–6.
23 S. W. Sawyer, M. E Oest, B. S Margulies and P. Soman, Behavior of encapsulated saos-2 cells within gelatin methacrylate hydrogels, *J. Tissue Sci. Eng.*, 2016, **7**(2), 1–7.
24 C. D O'Connell, C. Di Bella, F. Thompson, Ch. Augustine, S. Beirne, R. Cornock, Ch. J. Richards, J. Chung, S. Gambhir, Zh. Yue, J. Bourke, B. Zhang, A. Taylor, A. Quigley, R. Kapsa and P. Choong, Development of the biopen: a handheld device for surgical printing of adipose stem cells at a chondral wound site, *Biofabrication*, 2016, **8**(1), 015019.
25 X. Li, J. Zhang, N. Kawazoe and G. Chen, Fabrication of highly crosslinked gelatin hydrogel and its influence on chondrocyte proliferation and phenotype, *Polymers*, 2017, **9**, 309.
26 A. Nejadebrahim, M. Ebrahimi, X. Allonas, C. Croutxé-Barghorn, Ch. Leyb and B. Métralb, A new safranin based three-component photoinitiating system for high

resolution and low shrinkage printed parts *via* digital light processing, *RSC Adv.*, 2019, **9**, 39709–39720.

27 L. Liu, X. Li, X. Shi and Y. Wang, Injectable alendronate-functionalized GelMA hydrogels for mineralization and osteogenesis, *RSC Adv.*, 2018, **8**, 22764.

28 L. Li, C. Lu, L. Wang, M. Chen, J. White, X. Hao, K. M McLean and H. Chen, Gelatin-based photocurable hydrogels for corneal wound repair, *ACS Appl. Mater. Interfaces*, 2018, **10**(16), 13283–13292.

29 Ch. Fukay, Y. Nakayam, Y. Murayam, S. Omat, A. Ishikaw, Y. Hosak and T. Nakagaw, Improvement of hydrogelation abilities and handling of photocurable gelatin-based crosslinking materials, *J. Biomed. Mater. Res., Part B*, 2009, **91**(1), 329–336.

30 J. Y. Tan, C. K. Chua and K. F. Leong, Indirect fabrication of gelatin scaffolds using rapid prototyping technology, *Virtual Phys Prototyp*, 2010, **5**(1), 45–53.

31 Zh. Chen, Zh. Yu and G. Chen, Low-cost fabrication of poly(methyl methacrylate) microchips using disposable gelatin gel templates, *Talanta*, 2010, **81**, 1325–1330.

32 B. Huber, K. Borchers, G. Tovar and P. J. Kluger, Methacrylated gelatin and mature adipocytes are promising components for adipose tissue engineering, *J. Biomater. Appl.*, 2016, **30**(6), 699–710.

33 H. D. Woo, K. T. Park, E. H. Kim, Y. Heo, J. H. Jeong, D. G. Pyun, Ch. S. Choi, J. G. Lee, D. K. Han, J. W. Nah and T. Il Son, Preparation of UV-curable gelatin derivatives for drug immobilization on polyurethane foam: development of wound dressing foam, *Macromol. Res.*, 2015, **23**, 994–1003.

34 Y. Nakayama and T. Matsuda, Photocurable surgical tissue adhesive glues composed of photoreactive gelatin and poly(ethylene glycol) diacrylate, *J. Biomed. Mater. Res.*, 1999, **48**(4), 511–521.

35 S. Abdollahi Baghban, M. Khorasani and G. Mir Mohamad Sadeghi, Soundproofing flexible polyurethane foams: Effect of chemical structure of chain extenders on micro-phase separation and acoustic damping, *J. Cell. Plast.*, 2020, **56**(2), 167–185.

36 S. Abdollahi Baghban, M. Khorasani and G. Mir Mohamad Sadeghi, Soundproofing flexible polyurethane foams: the impact of polyester chemical structure on the microphase separation and acoustic damping, *J. Appl. Polym. Sci.*, 2018, **135**(46), 46744.

37 G. Irmak, T. Tolga Demirtaş and M. Gümüşderelioğlu, Highly methacrylated gelatin bio-ink for bone tissue engineering, *ACS Biomater. Sci. Eng.*, 2019, **5**(2), 831–845.

38 A. Duconseille, C. Gaillard, V. Santé-Lhoutellier and T. Astruc, Molecular and structural changes in gelatin evidenced by Raman microspectroscopy, *Food Hydrocolloids*, 2017, **77**, 777–786.

39 Th. Castagnet, A. Agirre, N. Ballard, L. Billon and J. M. Asua, Non-thermal microwave effects in radical polymerization of bio-based terpenoid (meth)acrylates, *Polym. Chem*, 2020, **11**, 6840–6846.

40 H. A. Brahmbhatt, A. Surtees, C. Tierney, O. A. Ige, E. V. Piletska and Th. Swift, Effect of polymerisation by microwave on the physical properties of molecularly imprinted polymers (MIPs) specific for caffeine, *Polym. Chem*, 2020, **11**, 5778–5789.

41 M. M. Babić, B. Đ. Božić, B. Đ. Božić, G. S. Uščumlić and S. Lj. Tomić, The innovative combined microwave-assisted and photo-polymerization technique for synthesis of the novel degradable hydroxyethyl (meth) acrylate/gelatin based scaffolds, *Mater. Lett.*, 2018, **213**, 236–240.

42 W. Tanan and S. Saengsuwan, Microwave Assisted Synthesis of Poly(Acrylamide-*co*-2-Hydroxyethyl Methacrylate)/ Poly(Vinyl Alcohol) Semi-IPN Hydrogel, *Energy Procedia*, 2014, **56**, 386–393.

43 L. Zhang, G. J. Zheng, Y. T. Guo, L. Zhou, J. Du and H. He, Preparation of novel biodegradable pHEMA hydrogel for a tissue engineering scaffold by microwave-assisted polymerization, *Asian Pac. J. Trop. Med.*, 2014, **7**, 36–140.

44 Th. Billiet, E. Gevaert, Th. D. Schryver, M. Cornelissen and P. Dubruel, The 3D printing of gelatin methacrylamide cell-laden tissue-engineered constructs with high cell viability, *Biomaterials*, 2014, **35**, 49–62.

45 K. S. Lim, B. S. Schon, N. V. Mekhileri, G. C. J. Brown, C. M. Chia, S. Prabakar, G. J. Hooper and T. B. F. Woodfield, New Visible-Light Photoinitiating System for Improved Print Fidelity in Gelatin-Based Bioinks, *ACS Biomater. Sci. Eng.*, 2016, **2**(10), 1752–1762.

46 C. H. Lin, K. F. Lin, K. Mar, S. Y. Lee and Y. M. Lin, Antioxidant *N*-acetylcysteine and glutathione increase the viability and proliferation of MG63 cells encapsulated in the gelatin-methacrylate/VA-086/blue light hydrogel system, *Tissue Eng., Part C*, 2016, **22**(8), 792–800.

47 R. Masuma, S. Kashima, M. Kurasaki and T. Okuno, Effects of UV wavelength on cell damages caused by UV irradiation in PC12 cells, *J. Photochem. Photobiol., B*, 2013, **125**, 202–208.

48 J. Hu, Y. Hou, H. Park, B. Choi, S. Hou, A. Chung and M. Lee, Visible light crosslinkable chitosan hydrogels for tissue engineering, *Acta Biomater.*, 2012, **8**(5), 1730–1738.

49 P. Occhetta, R. Visone, L. Russo, L. Cipolla, M. Moretti and M. Rasponi, VA-086 methacrylate gelatine photopolymerizable hydrogels: a parametric study for highly biocompatible 3D cell embedding, *J. Biomed. Mater. Res., Part A*, 2015, **103**(6), 2109–2117.

50 L. Shen, L. Zou, M. Ding, T. Zhao, L. Zhang and Q. Li, Molecular Dynamics Simulation on Dielectric Constant and Thermal Conductivity of Crosslink Epoxy/ functionalized graphene Nanocomposites, *Mater. Sci. Eng.*, 2020, **761**, 012009.

51 W. Li, Z. Zhang, Y. Zhai, L. Ruan, W. Zhang and L. Wu, Electrochemical and Computational Studies of Proline and Captopril as Corrosion Inhibitors on Carbon Steel in a Phase Change Material Solution, *Int. J. Electrochem. Sci.*, 2020, **15**, 722–739.

52 S. Choi, Y. Kim and H. Kim, Dielectric polymers for OTFT application, *J. Inf. Disp.*, 2010, **11**(3), 95–99.

53 K. J. Uwakwe, P. C. Okafor, A. I. Obike and A. I. Ikeuba, Molecular Dynamics Simulations and Quantum Chemical Calculations for the Adsorption of Some Imidazoline

Derivatives On Iron Surface, *Global J. Pure Appl. Sci.*, 2017, **23**, 69–80.

54 Z. Cheng, B. Yang, Q. Chen, Z. Shen and T. Yuan, Quantitative relationships between molecular parameters and reaction rate of organic chemicals in Fenton process in temperature range of 15.8–60 °C, *Chem. Eng. J.*, 2018, **350**, 534–540.

55 Z. Cheng, B. Yang, Q. Chen, X. Gao, Y. Tan, Y. Ma and Z. Shen, A Quantitative-Structure-Activity-Relationship (QSAR) model for the reaction rate constants of organic compounds during the ozonation process at different temperatures, *Chem. Eng. J.*, 2018, **353**, 288–296.

56 O. A. El-Gammal, A. F. Al-Hossainy and S. A. El-Brashy, Spectroscopic, DFT, optical band gap, powder X-ray diffraction and bleomycin-dependant DNA studies of Co(II), Ni(II) and Cu(II) complexes derived from macrocyclic Schiff base, *J. Mol. Struct.*, 2018, **1165**, 177–195.

57 U. Abdulfatai, A. Uzairu and S. Uba, Quantitative structure activity relationship study of anticonvulsant activity of α_substituted acetamido-*N*-benzylacetamide derivatives, *Cogent Chem.*, 2016, **2**(1), 1166538.

58 A. Jiang, Z. Cheng, Z. Shen and W. Guo, QSAR study on the removal efficiency of organic pollutants in supercritical water based on degradation temperature, *Chem. Cent. J.*, 2018, **12**, 12–16.

59 B. Yang, Z. Cheng, T. Yuan and Z. Shen, Denitrification of ammonia and nitrate through supercritical water oxidation (SCWO): a study on the effect of NO_3^-/NH_4^+ ratios, catalysts and auxiliary fuels, *J. Supercrit. Fluids*, 2018, **138**, 56–62.

60 B. Yang, Z. Shen, Z. Cheng and W. Ji, Total nitrogen removal, products and molecular characteristics of 14 N-containing compounds in supercritical water oxidation, *Chemosphere*, 2017, **188**, 642–649.

61 P. Su, H. Zhu and Z. Shen, QSAR models for removal rates of organic pollutants adsorbed by *in situ* formed manganese dioxide under acid condition, *Environ. Sci. Pollut. Res.*, 2016, **23**, 3609–3620.